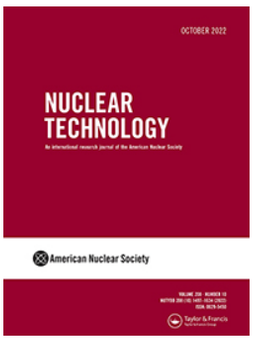

Nuclear Technology

ISSN: (Print) (Online) Journal homepage: https://www.tandfonline.com/loi/unct20

A New Method to Efficiently Estimate the Equilibrium State of Pebble Bed Reactors

Cihang Lu & Zeyun Wu

To cite this article: Cihang Lu & Zeyun Wu (2022) A New Method to Efficiently Estimate the Equilibrium State of Pebble Bed Reactors, Nuclear Technology, 208:10, 1577-1590, DOI: 10.1080/00295450.2022.2049966

To link to this article: https://doi.org/10.1080/00295450.2022.2049966

Published online: 18 May 2022.

NUCLEAR TECHNOLOGY · VOLUME 208 · 1577–1590 · OCTOBER 2022

DOI: https://doi.org/10.1080/00295450.2022.2049966

A New Method to Efficiently Estimate the Equilibrium State of Pebble Bed Reactors

Cihang Lu* and Zeyun Wu†

Virginia Commonwealth University, Department of Mechanical and Nuclear Engineering, 401 W. Main Street, Richmond, Virginia 23284-3015

Received December 29, 2021
Accepted for Publication February 28, 2022

Abstract — *Equilibrium state generation for the pebble bed reactor (PBR) is challenging due to the need to simultaneously account for both pebble movement and changes in fuel compositions. Multigroup diffusion codes have been historically employed to generate the equilibrium state and perform conventional neutronics calculations for PBRs, while neutron cross-section generation has been challenging due to the double heterogeneity of PBRs. Thanks to the capability to treat the double heterogeneity naturally, continuous-energy Monte Carlo (MC) methods are more suitable for detailed PBR analysis, but at the cost of significantly higher computing power.*

This paper presents a new Methodology to Efficiently Estimate the Equilibrium State of a PBR (MEEES-PBR) to generate equilibrium-state MC models for PBRs at lower computational expense. The MEEES-PBR is expected to contribute to the future development of PBR designs by accelerating the efforts in core designs and parametric studies. The theory of the MEEES-PBR is introduced in detail in this paper, and the procedure is demonstrated via an example application to the 165-MW(thermal) Xe-100 design. The computational cost and the accuracy of the MEEES-PBR are discussed to prove its viability.

Keywords — *Pebble bed reactor, equilibrium state, fuel composition distribution, Monte Carlo neutronics model.*

Note — *Some figures may be in color only in the electronic version.*

I. INTRODUCTION

The pebble bed reactor (PBR) has been under development for more than 6 decades. With the fuel pebbles continuously circulating, the PBR has high flexibility in fuel management and the capability of online refueling. More importantly, the PBR is commonly regarded with a distinct inherent safety due to the employment of TRISO particulate fuel—a tristructrual-isotropic particle consisting of a micro-spherical fuel material encapsulated by a series of coatings. The coatings of the TRISO fuel provide a buffer for fission gas deposition for the fuel particle and function as a miniature pressure vessel to minimize fission product release. The coated TRISO particles are randomly dispersed in a graphite matrix to construct the fuel pebble in the PBR. Although helium gas has been historically employed in the PBR as the coolant, such as in the AVR (Ref. 1), PBMR-400 (Ref. 2), and HTR-10 (Ref. 3), the use of molten salt as the coolant is also under active research, such as in the MK1-FHR (Ref. 4) and KP-FHR (Ref. 5).

Detailed neutronics analyses are indispensable for the future development of the PBR, but reactor physics calculations have been challenging for pebble bed–type reactors because of the need to account for both pebble movement and changes in fuel compositions at the same time. Different operational conditions can be identified for the PBR, including the running-in phase, where the characteristics of the core keep changing, and the equilibrium state,[6,7] where a quasi-static state is reached and all

*Current address: Nuclear Science and Technology Department, Brookhaven National Laboratory (clu@bnl.gov).
†E-mail: zwu@vcu.edu

the important parameters of the core remain constant. These include the pebble insertion and removal rate, the averaged fuel burnup (BU) at insertion and discharge, the temperature rising across the PBR, etc. The equilibrium state is characteristic for the largest part of the reactor operational conditions, and therefore is assumed for many performance and licensing calculations.[8] Equilibrium-state calculations can also provide effective initial conditions for most of the design-basis transient safety analyses.[9,10] Therefore, it is of paramount importance to obtain a PBR equilibrium state in the reactor calculations.

However, the current modeling of the equilibrium-phase state of a PBR usually requires large computational expense because repetitive fuel depletion calculations are required.[8,11] Although the continuous efforts made by researchers worldwide are leading to the emergence of numerous novel codes for PBR modeling,[12–14] historical VSOP (Ref. 15) and PEBBED (Ref. 16) are still the most widely used and credited codes to perform equilibrium-state calculations for the PBR. Both codes are multigroup diffusion codes despite the existing differences in algorithms and numerical techniques employed.[8] Because of the employment of TRISO fuel particles in the pebbles, the PBR is well known to bear the double-heterogeneous effect on neutronics aspect, which makes the neutron cross-section generation rather challenging for existing deterministic lattice codes. Conversely, the double heterogeneity can be naturally treated by the continuous-energy Monte Carlo (MC)–type methods that also have the capability of handling the complex geometries of advanced reactor systems.[17,18] These advantages make MC-based calculation tools the most suitable for detailed PBR core analyses.[19] However, due to the high requirement in computing power, the MC-based methods did not start to emerge until recent years. For example, based on the MC code MVP (Ref. 20), Setiadipura and Obara[21] developed a MC BU analysis code for PBRs (MCPBR), which can perform calculations for PBRs with the once-through-then-out (OTTO) fueling scheme.[18] Based on MCNP (Ref. 22), Fratoni and Greenspan[23] developed a three-dimensional full-core analysis methodology that is capable of simulating PBRs with multipass fueling schemes,[20] which was further improved by Cisneros.[24] Even with the high computational power available today, these MC calculations still take a long time to complete.

Motivated by the previous observations, a new Methodology to Efficiently Estimate the Equilibrium State of a PBR (MEEES-PBR) is developed in this work to generate the MC-based equilibrium models for the PBR. The philosophy of the MEEES-PBR is to divide the active core of a PBR into different fuel regions, estimate the equilibrium fuel BU in each fuel region, and then iteratively estimate the fuel compositions in each fuel region based on the BU value until both the effective multiplication factor k_{eff} and the BU distribution satisfy the specifications of the equilibrium core specifications. The fuel compositions corresponding to different BUs were obtained in advance by performing depletion calculations in a separate single-fuel-region model, in which only one fuel region with one single fuel material was considered. This single fuel material is considered as a reasonable representation of the "average" fuel in the core because any single fuel pebble in a PBR is not tracked and therefore has the equal probability to appear at any locations in the active core. It is pointed out that although the pebble-tracking methodology is not mature yet, both numerical[25,26] and experimental[27] efforts have been recently made by dedicated researchers to accelerate its realization. Besides the single-fuel-region model, another distinct feature of the MEES-PBR is that all calculations, including the depletion calculations, are performed with MC models, and thus the high order of model fidelity and computational accuracy are retained. As demonstrated by the application in this work, while being computational cost efficient, the MEEES-PBR provides a reasonable estimate of the fuel component distributions in equilibrium-state PBRs. The MEEES-PBR is expected to contribute to the future development of PBR designs by accelerating the efforts in core designs and optimization-oriented parametric studies, and it is not necessarily limited to gas-cooled PBRs.

The rest of this paper is organized as follows. Section II presents the theoretical basis and workflow of the MEEES-PBR. The main assumptions employed in the method are also thoroughly discussed in this section. Section III demonstrates the application of the MEEES-PBR by applying it in the analysis of X-energy's Xe-100 reactor design, and the computational cost of the application is detailed. In Sec. IV, several core characteristics of the Xe-100 design quantified by the MEEES-PBR are compared with existing references to show the accuracy of the MEEES. Section V summarizes the main efforts of this work and offers a brief perspective on future endeavors.

II. METHODOLOGY OF THE MEEES-PBR

For a better explanation of the MEEES-PBR, the active PBR core of interest is schematically illustrated in Fig. 1. The height of the cylindrical active core of the PBR of interest is noted as H, and the outer radius is noted as R. As shown in Fig. 1, the active core is divided into M concentric

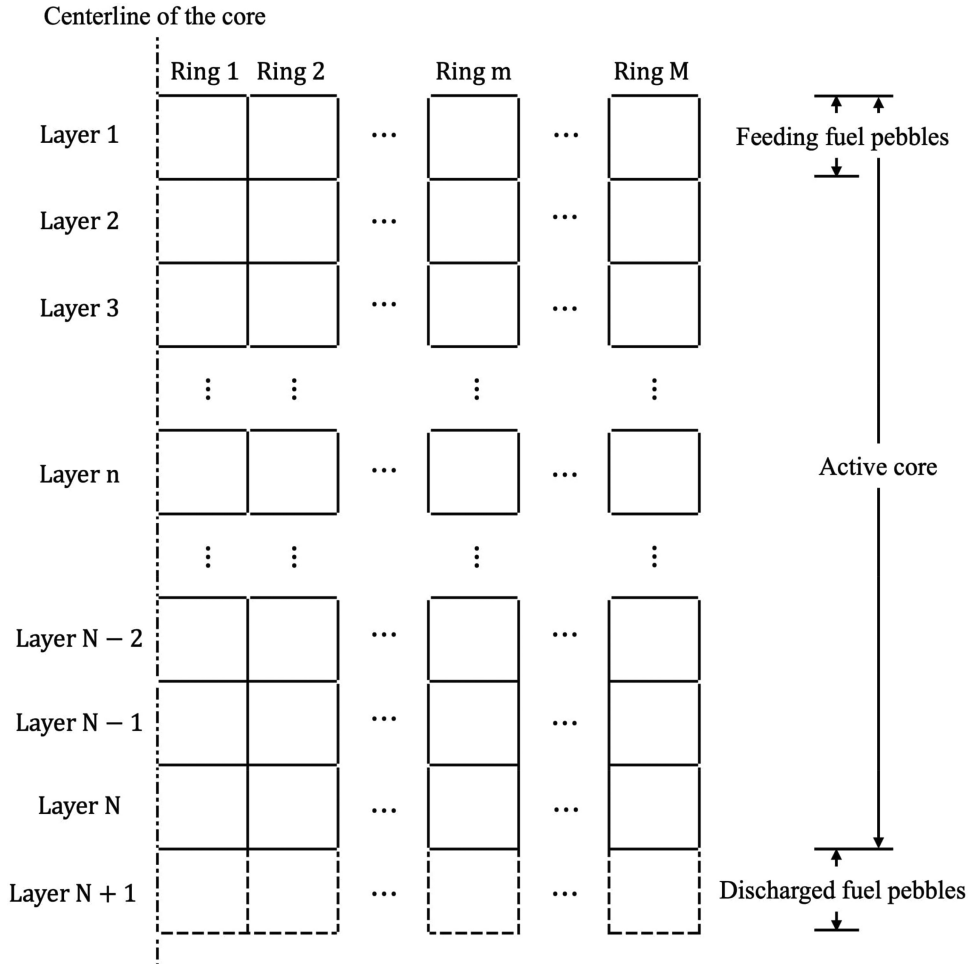

Fig. 1. Schematic of the active core of the PBR of interest in the MEEES.

fuel rings that are later referred to as the flow channels. Each fuel ring m has an outer radius of R_m, whereas $R_0 = 0$ and $R_M = R$. The active core is also divided into N equal-thickness fuel layers. Layer 1 is assumed to be filled with the feeding fuel pebbles, whereas layer $N + 1$, consisting of the discharged fuel pebbles, is located outside of the active core. Because the fuel pebbles are not tracked, their identities are lost when introduced into the active core of a PBR, and the fuel isotopic composition becomes the only characteristic to differentiate these fuel pebbles. At the equilibrium state, the distribution of the fuel isotopic composition is considered static in the active core, and the goal of the MEEES-PBR is to determine the fuel isotopic composition in each of the $M \times N$ fuel regions.

Because of the mixing of fuel pebbles when fed to the core, a specific fuel pebble has an equal possibility of being found at any location in the active core at the equilibrium state of a PBR, and each fuel pebble experiences the same neutron spectra during its depletion. It is therefore reasonable to consider that the fuel isotopic composition is directly correlated to the BU and to further assume that any two fuel pebbles with the same BU have the same fuel isotopic compositions. Therefore, the distribution of the fuel isotopic compositions that defines the equilibrium state of a PBR can be determined by finding the corresponding BU distribution. It is pointed out that the BU discussed previously does not refer to the depletion history of one single fuel pebble at one specific location of the active core where one specific neutron spectrum is experienced, but rather an "averaged" depletion history on which the different neutron spectra existing at all the locations of the active core have equal impact. The fuel isotopic composition as a function of the averaged BU can be determined by modeling the fuel in all the pebbles in the active core with a single material during the depletion calculation. An empirical approach used to estimate the average BU map for a specific reactor is described in Sec. II.A, followed by a detailed description of the MEEES-PBR procedure.

II.A. Estimate the Reactor-Specific Average BU Map

Fuel pebbles in the active core essentially move axially while their radial or azimuthal movement is relatively limited.[20,24] The fuel pebbles have more significant nonaxial flow near the bottom of the core, when redirected by the cone to the discharge chute.[28] However, this effect was neglected because we did not consider the bottom cone and discharge chute of the PBR in the MEEES-PBR for simplicity. This simplification was not expected to have a significant impact on the neutron flux distribution in the core because the neutron fluxes at these regions were small.[21] Therefore, we assumed that the pebbles only moved within their flow channels in the MEEES-PBR. By assuming the fuel pebbles in direct contact with the wall of the active core to be static, the pebble flow velocity v_r was modeled as a second-order polynomial of its distance to the centerline of the core[8] as

$$v_r = a(R - r)^2, \tag{1}$$

where a is an arbitrary constant that will be canceled later. By assuming a uniform packing fraction (PF) of the fuel pebbles in the active core, the volumetric flow rate of the fuel pebbles in ring m was calculated as

$$Q_m = \int_{R_{m-1}}^{R_m} \mathrm{PF} \cdot a(R - r)^2 \cdot 2\pi r dr. \tag{2}$$

The averaged pebble velocity in ring m was therefore

$$v_m = \frac{Q_m}{A_m} = PF \cdot a \cdot \frac{\left[R^2 r^2 - 4/3 \cdot Rr^3 + 1/2 \cdot r^4\right]_{R_{m-1}}^{R_m}}{\left[r^2\right]_{R_{m-1}}^{R_m}}. \tag{3}$$

The total increase of fuel BU in ring m throughout the active core ΔBU_m was expressed as

$$\Delta \mathrm{BU}_m = b \cdot \frac{H}{v_m} = \frac{bHA_m}{Q_m} \tag{4}$$

by assuming a linear BU increasing rate b. The averaged increment of BU throughout the core per pass of the fuel pebbles was therefore

$$\Delta BU_{averaged} = \frac{\sum_{m=1}^{M} Q_m \Delta BU_m}{\sum_{m=1}^{M} Q_m} = b \cdot \frac{H \sum_{m=1}^{M} A_m}{\sum_{m=1}^{M} Q_m}. \tag{5}$$

The averaged increment of BU per pass should be given in the specifications of each reactor design. For example, the 10-MW(thermal) HTR-10 design has an averaged fuel BU of 80MWd/kgHM per five passes,[3] which means a $\Delta BU_{averaged} = 16$MWd/kgHM per pass. The Mark-1 PB-FHR (fluoride-cooled high-temperature reactor) design has an averaged fuel BU of 180MWd/kgHM per eight passes,[4] which means a $\Delta BU_{averaged} = 22.5$MWd/kgHM per pass, etc. With $\Delta BU_{averaged}$ specified, the coefficient b in Eq. (5) was calculated as

$$b = \Delta BU_{averaged} \cdot \frac{\sum_{m=1}^{M} Q_m}{H \sum_{m=1}^{M} A_m}, \tag{6}$$

and the BU in fuel ring m and fuel layer n was

$$BU_{m,n} = BU_{feeding} + \Delta BU_{averaged} \cdot \frac{n-1}{N} \cdot \frac{A_m}{Q_m} \cdot \frac{\sum_{m=1}^{M} Q_m}{\sum_{m=1}^{M} A_m}. \tag{7}$$

Note the coefficients a and b and the fuel pebble PF were canceled out in Eq. (7), and Eq. (7) is the one used to estimate the reactor-specific BU distribution in the MEEES-PBR.

II.B. MEEES-PBR Procedure

Based on the considerations and estimations outlined previously, the MEEES-PBR can be implemented with the following six steps through a MC modeling and simulation tool:

Step 1. Build a MC model for the PBR core under investigation according to the reactor specifications. This model is high fidelity because every TRISO particle and every fuel pebble are explicitly modeled. Only one fuel material is used to represent the average fuel in the core, and the model is referred to as the single-fuel-region model. The single-fuel-region model is established with fresh fuel at this step and used for depletion calculations in step 4 to provide a reactor-specific BU database for the MEEES-PBR.

Step 2. Select the number of fuel rings M and the number of fuel layers N, and then divide the active core into $M \times N$ fuel regions.

Step 3. Calculate the fuel $BU_{m,n}$ in each of the fuel regions by using Eq. (7). In case the OTTO fueling scheme is used, the feeding fuel pebbles have a $BU_{feeding}$ of 0; in case a multipass fueling scheme is used, the $BU_{feeding}$ will be 0 as the initial guess and will be adjusted later according to the k_{eff} specified in the reactor specifications.

Step 4. Perform depletion calculations with the single-fuel-region model established in step 1 and output the fuel isotopic compositions at each of the $BU_{m,n}$ identified in step 3.

Step 5. Construct the multifuel-region model based on the single-fuel-region model by defining each fuel region with the fuel isotopic compositions determined in step 4.

Step 6. Output the multifuel-region model if the k_{eff} fits the specified equilibrium-state k_{eff} within the user-defined tolerance ε. If not, adjust the $BU_{feeding}$ properly and go back to step 3.

To facilitate the understanding of the MEEES-PBR method, a flow chart illustrating the equilibrium core estimate procedure is shown in Fig. 2.

It is pointed out that when adjusting the $BU_{feeding}$ to get the specified equilibrium-state k_{eff}, one depletion calculation is needed in each iteration to calculate the fuel isotopic composition at the corresponding $BU_{m,n}$. However, to reduce computational cost, high precision is not sought for these depletion calculations. Low active neutron history numbers can be employed in the first place, and a depletion calculation with more active neutron histories should be performed when the $BU_{feeding}$ that leads to the specified equilibrium-state k_{eff} is identified.

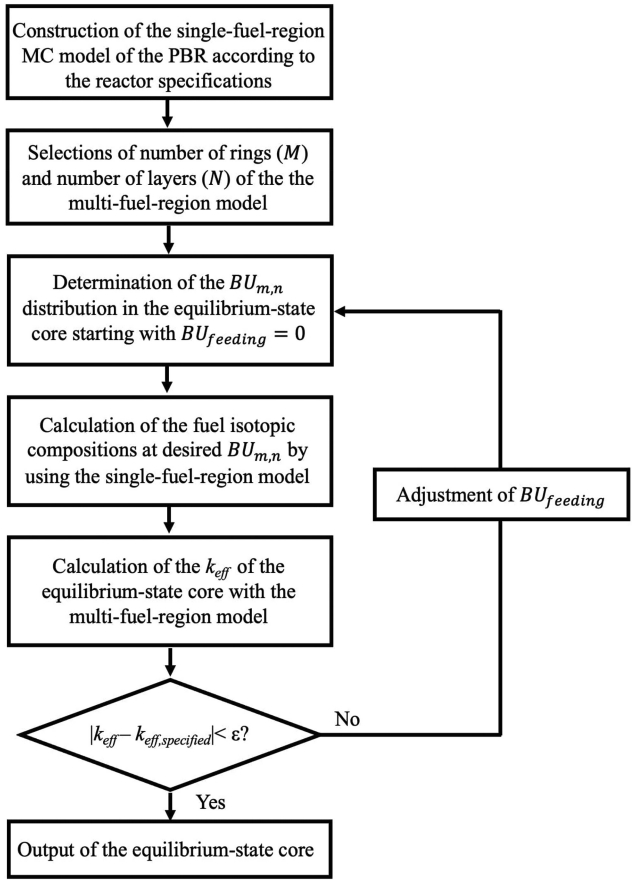

Fig. 2. Flow chart of the MEEES-PBR.

II.C. MEEES-PBR Limitations

In the course of the MEEES-PBR development, the main assumptions being made along the procedure are summarized as follows:

1. The fuel pebbles are well mixed when fed to the core.

2. The isotopic composition of all the fuel pebbles in the same fuel region is the same.

3. Fuel pebbles in the active core only move axially. The flow velocity is a second-order polynomial of its distance to the centerline of the core, whereas the fuel pebbles in contact with the wall of the active core are static.

4. Any two fuel pebbles with the same BU have the same fuel isotopic compositions.

5. The BU is proportional to the pebble residence time in the core.

6. The fuel isotopic composition calculated by depleting the sing-fuel-region model can be considered as the fuel isotopic composition at specific averaged BU.

7. A constant fuel temperature of 900 K and a constant nonfuel temperature 600 K were applied throughout the MC calculation.

The application of the MEEES-PBR may be limited considering different core designs due to the previous assumption. For example, the assumption that fuel BU is proportional to the pebble residence time in the core gets less valid when the BU gets higher. Therefore, estimating the BU gain per pass by dividing the discharge BU by total pass number may cause more significant errors when the BU is larger. Also, because of the different neutron spectrum hardnesses seen at different locations in the core, two

fuel pebbles with the same BU may have different isotopic compositions, etc. It is speculated that the accuracy of the MEEES-PBR gets worse for the cores that are larger, that have more complicated geometries, and that have larger discharge BU. Although these limitations were acceptable in this study as we considered an averaged BU rather than focusing on the single fuel pebbles, they are worth investigating in more details in our future work.

III. APPLICATION OF THE MEEES-PBR

X-energy is a nuclear reactor and fuel design engineering company located in Rockville, Maryland. X-energy was recently awarded $80 million by the U.S. Department of Energy's Advanced Reactor Demonstration Program as the initial funding to build a commercial-scale pebble-bed-type gas-cooled reactor, named Xe-100, by 2028 as expected. The procedure of the MEEES-PBR is demonstrated in this section via an application of the method to the 165-MW(thermal) Xe-100 design,[28] the detailed specifications of which provided a reliable reference solution resource to verify the proposed method. A schematic of the 165-MW(thermal) Xe-100 design is shown in Fig. 3.

III.A. Single-Fuel-Region Model

We built the single-fuel-region model of the 165-MW (thermal) Xe-100 according to the specifications summarized in Table I by using the MC neutronics code Serpent[29] and employing the ENDF/B-VII.0 library. The single-fuel-region model was started with a fresh fuel and depleted to provide the BU database of the average fuel for the MEEES-PBR method.

In the single-fuel-region model, each fuel pebble contained 19 542 identical TRISO fuel particles such that the uranium loading per pebble was 7 g. These TRISO particles were randomly distributed in the center part of each fuel pebble by leaving an outer fuel-free zone with a thickness of 5 mm, as shown in Fig. 4. The fuel kernels were modeled as $UC_{0.5}O_{1.5}$ with a ^{235}U enrichment of 15.5 wt %, whereas a constant temperature of 900 K was applied to all the fuel materials. The other materials were modeled at a constant temperature of 600 K.

According to the Xe-100 specifications, we filled the core of the single-fuel-region model with 223 039 fuel pebbles that were considered to have the same TRISO particle distributions for simplicity. We assumed that the fuel pebbles were densely packed in the core and constructed the active core by repeating the hexagonal closest packing unit cells, which is a common approach employed to model the fuel pebbles.[30] Two types of control rods (CRs) were modeled in the single-fuel-region model, namely, the reactivity control system (RCS) and the reserve shutdown system (RSS). The RCS had a maximum insertion length of 660 cm, and the RSS had a maximum insertion length of 860 cm. With a diameter of 13 cm, both types of CRs consisted of 8-mm-thick annular B_4C compacts stacked in Incoloy-800H (Ref. 31) canisters, which had an inner radius of

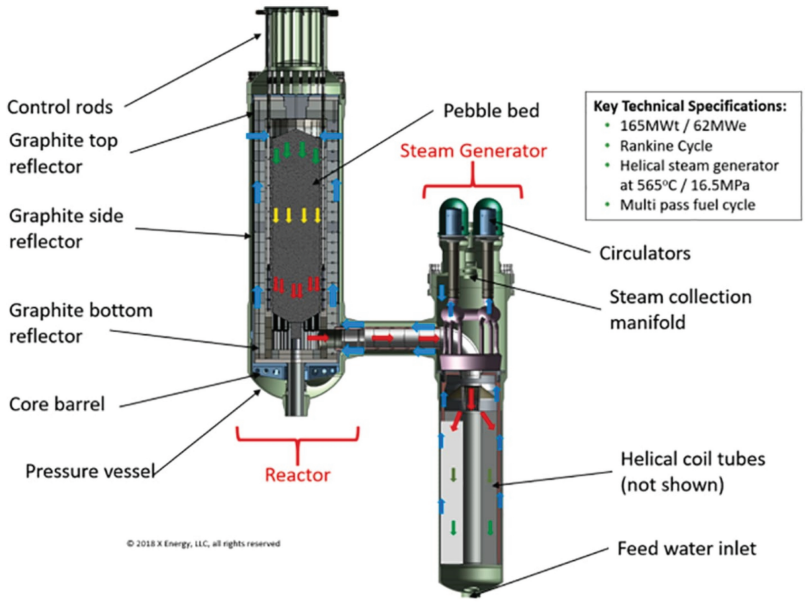

Fig. 3. Schematic of the 165-MW(thermal) Xe-100 reactor.[28]

TABLE I

Specifications of the 165-MW(thermal) Xe-100 Design*

	Parameter	Value	Unit
Core geometric specifications	RPV diameter	4.88	Meter
	Core diameter	2.4	Meter
	Core height	8.93	Meter
	Chute diameter	0.5	Meter
Fuel pebble specifications	Pebble diameter	6	Centimeter
	Uranium loading per pebble	7	Gram
	^{235}U enrichment	15.5	wt%
	Fuel pebbles in the core	223 000	–
Fueling scheme	Equilibrium-state k_{eff}	1.0015	–
	Average BU at discharge	165	MWd/kgHM
	Number of passes	6	–

*Reference 28.

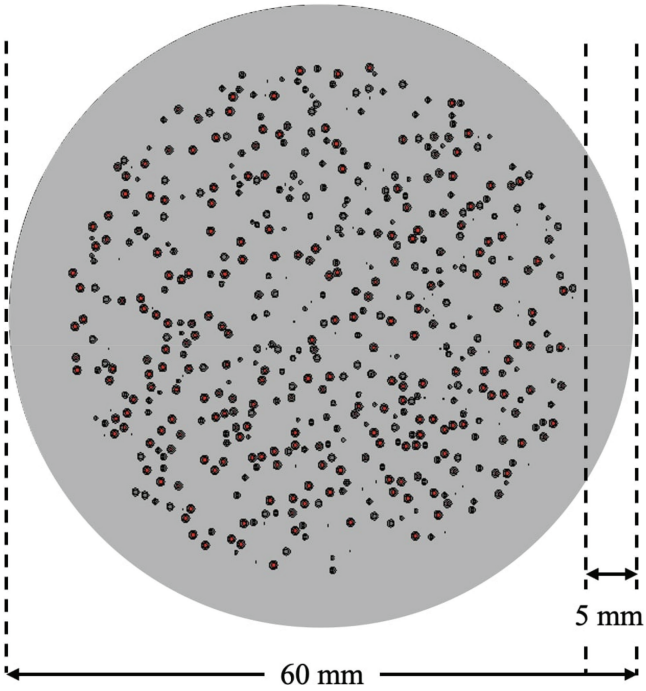

Fig. 4. Cross-sectional view of a fuel pebble with randomly distributed TRISO particles.

41.5 mm, an inner wall thickness of 0.5 mm, and an outer wall thickness of 2.5 mm. The CR borings were located inside the reflector at around 10 cm away from the active core.[32] Figure 5 shows the cross-sectional views of the single-fuel-region model with the locations of the 18 CRs (9 for the RCS and 9 for the RSS) marked. Because the single-fuel-region model was initiated with completely fresh fuel pebbles, it had an all-rods-out k_{eff} of 1.38023 (±10 pcm). This value is not comparable with the specified equilibrium-state k_{eff} (1.0015) of the 165-MW (thermal) Xe-100 design,[28] but is given here to inform about the large excessive reactivity of the fresh core.

III.B. Multifuel-Region Model

We built the multifuel-region model of the 165-MW (thermal) Xe-100 based on the single-fuel-region model by applying the MEEES-PBR method described in Sec. II. We selected four concentric fuel rings ($M = 4$) and ten fuel layers ($N = 10$), and divided the active core of the model into 40 fuel regions, as depicted in Fig. 6. In the multifuel-region model, we assumed the fuel pebbles located in the bottom cone and the discharge chute to have the same BU as those located in layer 10 because they have a minor impact on the neutron flux of the core.[21] The fuel pebbles of the 165-MW (thermal) Xe-100 design had an averaged BU increment per pass of $\Delta BU_{averaged} = 27.5\text{MWd/kgHM}$, as the total BU gained through six passes was 165 MWd/kgHM (Ref. 28). The BUs in each of the fuel regions were calculated by calling Eq. (7), assuming that fuel layer 1 contained feeding fuel pebbles only. The increment of the BU in each fuel region is summarized in Fig. 7. The $BU_{feeding}$ that fit the k_{eff} of the multifuel-region model with the specified equilibrium-state k_{eff} of the 165-MW(thermal) Xe-100 design was determined by repeating steps 3 through 6 of the MEEES-PBR as introduced in Sec. II.

The equilibrium state of the Kairos Power Fluoride Salt-Cooled, High Temperature Reactor (KP-FHR) was defined by using 88 isotopes.[33] Although different coolants were used in the KP-FHR and Xe-100, the fuel isotopes were expected to have similar importance in these two reactor designs because they both employ thermal neutron spectra and similar pebble fuel forms. Therefore, the same 88 isotopes were

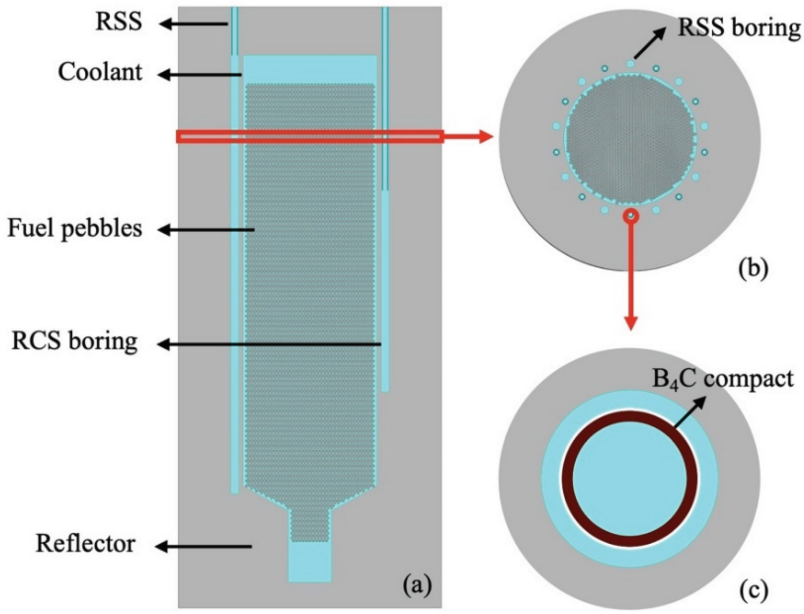

Fig. 5. (a) Vertical and (b) horizontal cross-sectional views of the single-fuel-region model, and (c) the zoom view of an RCS boring with CR inserted.

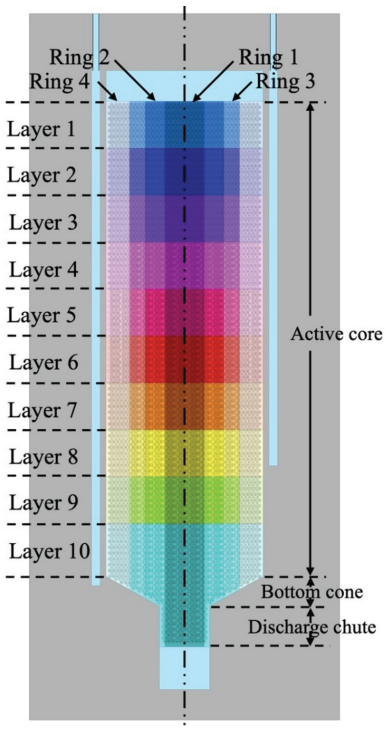

Fig. 6. The 40 fuel regions defined in the multifuel-region model.

tracked in this work when performing depletion calculations with the single-fuel-region model. The $BU_{feeding} = 90\text{MWd/kgHM}$ that led to a k_{eff} of 1.00233, which agreed with the specified value of the 165-MW(thermal) Xe-100 design (1.0015) within a tolerance of $\varepsilon = 100\,\text{pcm}$, was obtained in five iterations. The k_{eff} of the multifuel-region model as a function of the $BU_{feeding}$ investigated is summarized in Fig. 8. Each MC calculation employed 4×10^5 active neutron histories before the determination of the $BU_{feeding}$, whereas confirmatory calculations employed 4×10^6 active neutron histories each after the determination of the $BU_{feeding}$. The detailed computational cost and the associated k_{eff} uncertainties of the MC calculations performed are summarized in Table II. The whole MEEES-PBR procedure to finalize the multifuel-region model of the 165-MW(thermal) Xe-100 was completed within 77 h by using forty-five 2.5-GHz processor cores. In comparison, Fratoni and Greenspan's method[23] took about 360 h to establish a whole-core equilibrium model (represented by 1000 fuel pebbles) with twenty 2.8-GHz processor cores. The efficiency of the MEEES-PBR should be further confirmed when more PBR MC modeling studies become available in the literature. The distributions of three fissile isotopes in the multifuel-region model, namely ^{235}U, ^{239}Pu, and ^{241}Pu, are summarized in Fig. 9 for future verifications when experimental data become available or when comparable studies are performed.

IV. EVALUATION OF THE MEEES-PBR

Several important characteristics of the equilibrium-state 165-MW(thermal) Xe-100 were quantified with the multifuel-region model and compared with the reference calculations to evaluate the accuracy of the MEEES-PBR.

	Ring 1	Ring 2	Ring 3	Ring 4
Layer 1	$BU_{feeding}$	$BU_{feeding}$	$BU_{feeding}$	$BU_{feeding}$
Layer 2	+0.7	+1	+3	+24
Layer 3	+1	+2	+7	+47
Layer 4	+2	+4	+10	+71
Layer 5	+3	+5	+13	+95
Layer 6	+3	+6	+16	+118
Layer 7	+4	+7	+20	+142
Layer 8	+5	+8	+23	+166
Layer 9	+5	+10	+26	+189
Layer 10	+6	+11	+30	+213

Fig. 7. Equilibrium-state increment of BU (in MWd/kgHM) in the multifuel-region model.

The characteristics investigated in this section included the vertical and horizontal neutron flux distributions, the integral CR worth, and the reactivity temperature coefficients (RTCs).

The reference calculations of the 165-MW(thermal) Xe-100 considered in this paper were performed by Mulder and Boyes[28] by using the system of design diffusion code VSOP-A developed at X-energy.[34] The ENDF/B-VII library was employed, and the neutron fluxes were structured into four groups, namely, the thermal flux group ($E < 1.86$ eV), the epithermal-1 flux group (1.86eV $< E <$ 29eV), the epithermal-2 flux group (29eV $< E <$ 0.1MeV), and the fast flux group ($E >$ 0.1MeV). Figure 10 compares the geometry of the VSOP-A model with that of the multifuel-region model developed in this paper.

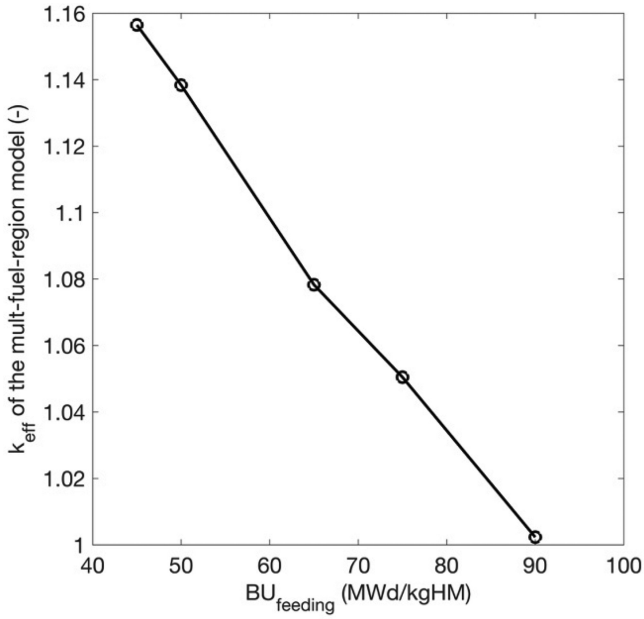

Fig. 8. k_{eff} of the multifuel-region model as a function of $BU_{feeding}$.

The vertical neutron flux distributions calculated by using both models are compared in Fig. 11. Both the magnitudes and the shapes of the fluxes had good agreement, whereas the peaks of both the fast and the thermal flux were located at slightly higher locations in the multifuel-region model. This implied that compared to the VSOP-A model, the BUs were overestimated at lower locations in the multifuel-region model. The radial neutron fluxes normalized to

TABLE II

Detailed Computational Cost and the Uncertainties of the MEEES-PBR

Stage	Model	Depletion Steps	Iterations	Active Neutron Histories	Uncertainty in k_{eff} (pcm)	Computational Time (h)
Seeking $BU_{feeding}$	Single-fuel-region	~30	5	$4 \cdot 10^5$	60	42
	Multifuel-region	1	5	$4 \cdot 10^5$	135	0.25
Confirmatory	Single-fuel-region	~30	1	$4 \cdot 10^6$	30	33
	Multifuel-region	1	1	$4 \cdot 10^6$	50	1.3

	Ring 1		Ring 2		Ring 3		Ring 4	
Layer 1	U235	0.432	U235	0.432	U235	0.432	U235	0.432
	Pu239	0.066	Pu239	0.066	Pu239	0.066	Pu239	0.066
	Pu241	0.015	Pu241	0.015	Pu241	0.015	Pu241	0.015
Layer 2	U235	0.427	U235	0.427	U235	0.415	U235	0.300
	Pu239	0.066	Pu239	0.066	Pu239	0.066	Pu239	0.063
	Pu241	0.015	Pu241	0.015	Pu241	0.016	Pu241	0.019
Layer 3	U235	0.427	U235	0.421	U235	0.392	U235	0.193
	Pu239	0.066	Pu239	0.066	Pu239	0.066	Pu239	0.058
	Pu241	0.015	Pu241	0.016	Pu241	0.016	Pu241	0.021
Layer 4	U235	0.421	U235	0.409	U235	0.375	U235	0.103
	Pu239	0.066	Pu239	0.066	Pu239	0.065	Pu239	0.050
	Pu241	0.016	Pu241	0.016	Pu241	0.017	Pu241	0.020
Layer 5	U235	0.415	U235	0.403	U235	0.359	U235	0.044
	Pu239	0.066	Pu239	0.066	Pu239	0.065	Pu239	0.045
	Pu241	0.016	Pu241	0.016	Pu241	0.018	Pu241	0.018
Layer 6	U235	0.415	U235	0.398	U235	0.342	U235	0.014
	Pu239	0.066	Pu239	0.066	Pu239	0.065	Pu239	0.039
	Pu241	0.016	Pu241	0.016	Pu241	0.018	Pu241	0.015
Layer 7	U235	0.409	U235	0.392	U235	0.321	U235	0.003
	Pu239	0.066	Pu239	0.066	Pu239	0.064	Pu239	0.036
	Pu241	0.016	Pu241	0.016	Pu241	0.019	Pu241	0.014
Layer 8	U235	0.403	U235	0.386	U235	0.305	U235	0.001
	Pu239	0.066	Pu239	0.066	Pu239	0.063	Pu239	0.033
	Pu241	0.016	Pu241	0.017	Pu241	0.019	Pu241	0.013
Layer 9	U235	0.403	U235	0.375	U235	0.290	U235	0.000
	Pu239	0.066	Pu239	0.065	Pu239	0.063	Pu239	0.032
	Pu241	0.016	Pu241	0.017	Pu241	0.019	Pu241	0.012
Layer 10	U235	0.398	U235	0.370	U235	0.270	U235	0.000
	Pu239	0.066	Pu239	0.065	Pu239	0.062	Pu239	0.031
	Pu241	0.016	Pu241	0.017	Pu241	0.020	Pu241	0.012

Fig. 9. Mass distribution of ^{235}U, ^{239}Pu, and ^{241}Pu (in g/pebble) in the multifuel-region model.

their maximum values are compared in Fig. 12. The distributions of the fast fluxes had very good agreement, and the thermal fluxes peaked at the same radial location. However, the normalized thermal flux calculated by the multifuel-region model had a higher magnitude around the center of the core, which suggested a better moderation capability predicted by the multifuel-region model at the corresponding locations.

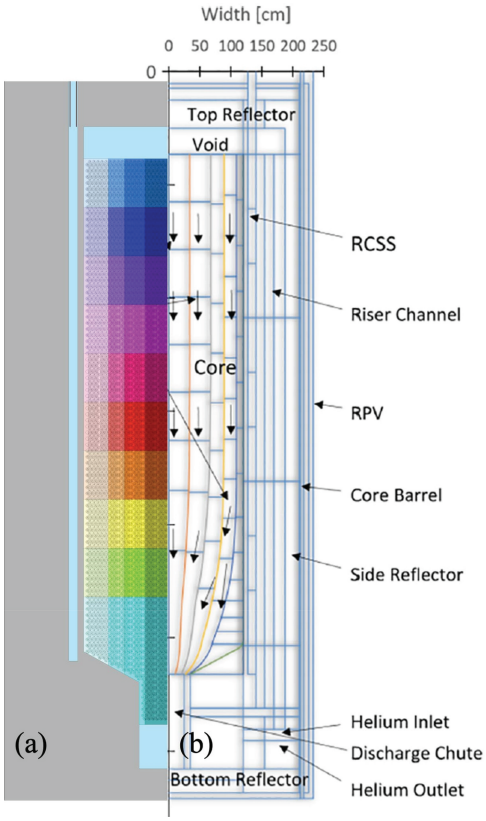

Fig. 10. Comparison between (a) the multifuel-region model and (b) the VSOP-A model[28] of the 165-MW (thermal) Xe-100 design.

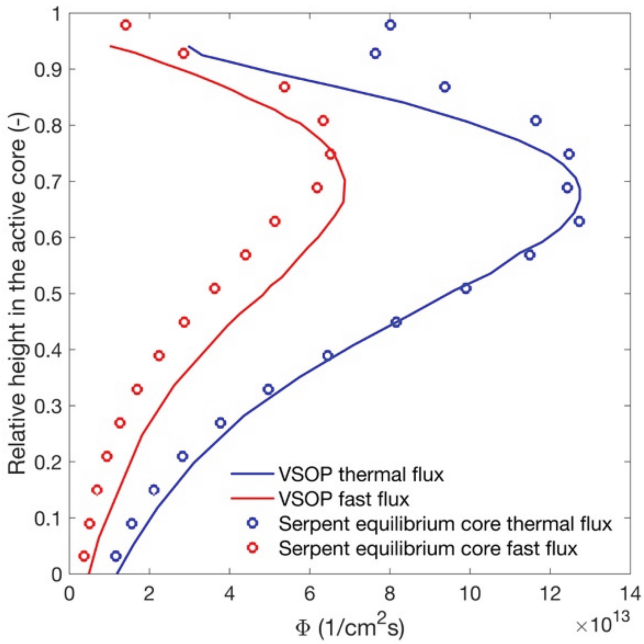

Fig. 11. Comparison between the vertical neutron flux distributions.

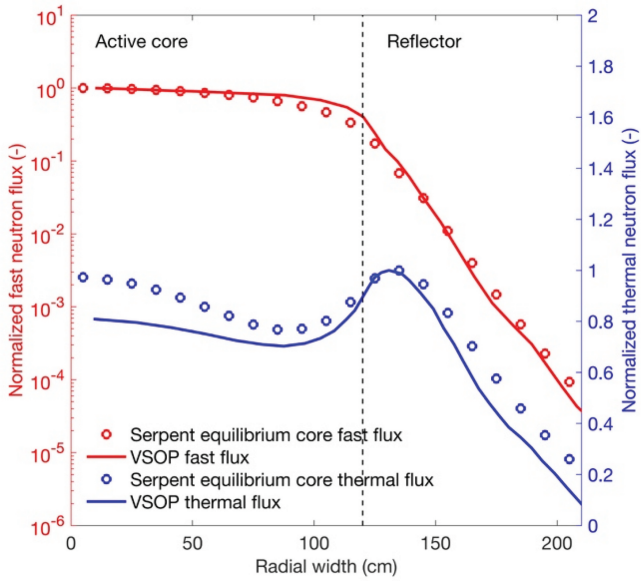

Fig. 12. Comparison between the normalized radial neutron flux distributions.

By using the multifuel-region model, we calculated the integral CR worth as the difference between the k_{eff} of the core with all CRs withdrawn and that with the CRs inserted to different lengths. The nine CRs of the same type were modeled to move at the same time. The integral CR worth calculated had an associated uncertainty of ±100 pcm because each MC calculation had an associated uncertainty of ±50 pcm. The worth of the RSS was minor in the overlap region with the RCS because the former was calculated by considering that the RCS was completely inserted. While the integral CR worth of the RCS calculated with both models generally had a good agreement, that of the RSS calculated with the multifuel-region model had a systematic underestimation of around 1000 pcm, as shown in Fig. 13. Also, the discrepancies became larger at the lower part of the core for both types of CRs. This again implied that compared to the VSOP-A model, the BUs were overestimated in the multifuel-region model, which decreased the neutron flux and the ensuing integral CR worth.

We investigated three RTCs, including the Doppler coefficient, the moderator temperature coefficient, and the reflector temperature coefficient. The temperatures of the fuel, moderator, and reflector were set to 300, 600, 900, and 1200 K, and the coefficients were calculated by using Eq. (8):

$$\mathrm{RTC}(T) = \frac{k_{eff}(T + 150\mathrm{K}) - k_{eff}(T - 150\mathrm{K})}{300\mathrm{K}}. \qquad (8)$$

Because each k_{eff} had an uncertainty of ±50 pcm, the RTC quantified with Eq. (8) had an uncertainty of

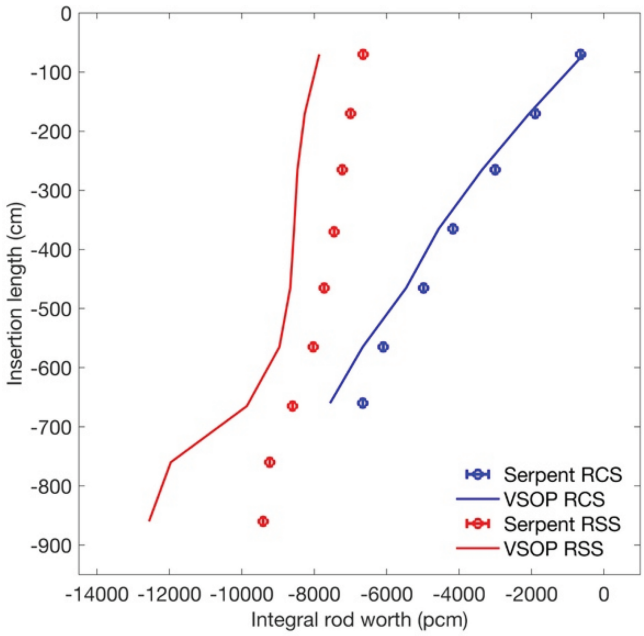

Fig. 13. Comparison between the integral CR worth calculated with both models.

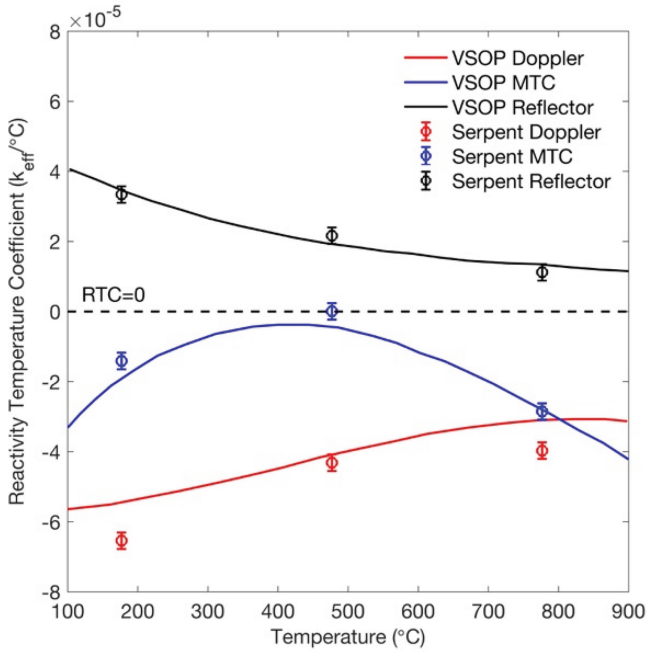

Fig. 14. Comparison between the RTCs calculated with both models.

±0.25 pcm/K according to the propagation of the uncertainties. The RTC calculated with both codes had a very good agreement, as shown in Fig. 14. Other temperatures can also be assigned to the materials to calculate the corresponding RTC besides the four investigated in this study. However, in the Serpent code the ENDF library only provides nuclear data at these four PBR-relevant temperatures. The neutron cross sections at other temperatures are obtained through linear interpolation, and the corresponding RTC calculated will therefore not be as accurate. It is noted that changes in the mass density of materials were not considered in the calculation of the RTC in this study, which may contribute to the observed discrepancies.

V. SUMMARY AND FUTURE WORK

The MEEES-PBR was developed in this work to support the future development of PBR technologies. While leveraging the advantages of MC methods in taking care of the double heterogeneity, the MEEES-PBR also largely decreases the computing time required by MC methods such that the research in PBR core designs and parametric studies can be accelerated.

The theory of the MEEES-PBR was introduced in detail in this paper, and the procedure was demonstrated via an example application to the 165-MW(thermal) Xe-100 design. The total computational cost to build the multifuel-region model with the MEEES-PBR was 77 h of calculation time with forty-five 2.5-GHz processor cores, which was more than 50% more efficient than the existing MC methods. Because no experimental data exist yet, several core characteristics quantified with the multifuel-region model were compared to the reference calculations of the 165-MW(thermal) Xe-100 performed with VSOP-A to evaluate the accuracy of the MEEES-PBR. Although discrepancies exist, the characteristics calculated with both models generally had good agreement, which proved the good viability of the MEEES-PBR. In future studies, the MEEES-PBR will be applied to other PBR designs and the results will be evaluated to further confirm the conclusion made previously.

Along with the procedures of the MEEES-PBR, the following assumptions were identified and emphasized to ensure the validity of the method:

1. The fuel pebbles were well mixed when fed to the core.

2. The isotopic composition of all the fuel pebbles in the same fuel region was the same.

3. Fuel pebbles in the active core only moved axially. The flow velocity was a second-order polynomial of its distance to the centerline of the core, whereas the pebbles in contact with the wall of the active core were static.

4. Any two fuel pebbles with the same BU had the same fuel isotopic composition.

5. The fuel BU was proportional to the pebble residence time in the core.

6. The fuel isotopic composition calculated by depleting the single-fuel-region model was considered as the fuel isotopic composition at specific averaged BU.

7. A constant fuel temperature of 900 K and a constant nonfuel temperature of 600 K were applied throughout the MC calculation.

As a result, uncertainty quantification is anticipated in future studies to understand the uncertainties caused by the assumptions outlined previously. Two progressive goals are expected to be achieved by performing the uncertainty analysis: (1) We will quantify the uncertainties caused by the employment of the MEEES-PBR, and (2) we will identify the most significant source of uncertainties and modify the assumptions accordingly to improve the accuracy of the MEEES-PBR. We will also perform probabilistic research to characterize the stochastic path that the fuel pebbles may take to further enhance the ΔBU estimation.

Additionally, while 40 fuel regions were employed in the example application in this paper, increasing the number of fuel regions may increase the accuracy of the MEEES-PBR. We will therefore perform sensitivity analyses in the future considering the selections of M and N, such that the accuracy of the model can be improved while keeping the computational cost acceptable.

Acknowledgments

The authors would like to thank Eben Mulder and Sonat Sen from X-energy for technical discussions on the Xe-100 model at the initial stage of this study. The authors are also grateful to the two anonymous reviewers of this manuscript for their constructive comments and suggestions during the preparation of the manuscript.

Disclosure Statement

No potential conflict of interest was reported by the authors.

ORCID

Cihang Lu http://orcid.org/0000-0002-6385-6338
Zeyun Wu http://orcid.org/0000-0002-6114-0352

References

1. K. J. KRUEGER and G. P. IVENS, "Safety-Related Experiences with the AVR Reactor," presented at the Specialists' Mtg. on Safety and Accid. Anal. for Gas-Cooled Reactors, Oak Ridge, Tennessee, May 13–15, 1985, p. 61 (IAEA-TECDOC-358) (1985).

2. G. STRYDOM et al., "The OECD/NEA/NSC PBMR 400 MW Coupled Neutronics Thermal Hydraulics Transient Benchmark: Transient Results," presented at PHYSOR 2010, Pittsburgh, Pennsylvania, May 9–14, 2010.

3. Z. WU, D. LIN, and D. ZHONG, "The Design Features of the HTR-10," *Nucl. Eng. Des.*, **218**, *1–3*, 25 (2002); https://doi.org/10.1016/S0029-5493(02)00182-6.

4. A. T. CISNEROS et al., "Technical Description of the "Mark 1" Pebble-Bed Fluoride-Salt-Cooled High-Temperature Reactor (PB-FHR) Power Plant," Tech. Rep., University of California, Berkeley, Department of Nuclear Engineering, (2014).

5. E. BLANDFORD et al., "Kairos Power Thermal Hydraulics Research and Development," *Nucl. Eng. Des.*, **364**, 110636 (2020); https://doi.org/10.1016/j.nucengdes.2020.110636.

6. Z. WU and R. E. WILLIAMS, "A Fast and Self-Consistent Approach for Multi-cycle Equilibrium Core Studies Using Monte Carlo Models," presented at the Joint Int. Conf. on Math. and Comput. (M&C), Supercomputing in Nucl. Appl. (SNA) and the Monte Carlo (MC) Method, Nashville, Tennessee, April 19–23, 2015.

7. Z. WU et al., "A Core Design for a Small Modular Boiling Water Reactor with Long-Life Core," *Nucl. Technol.*, **193**, *3*, 364 (2016); https://doi.org/10.13182/NT15-58.

8. H. D. GOUGAR, F. REITSMA, and W. JOUBERT, "A Comparison of Pebble Mixing and Depletion Algorithms Used in Pebble-Bed Reactor Equilibrium Cycle Simulation," *Proc. 2009 Int. Conf. on Math., Comput. Methods, and Reactor Phys.*, Saratoga Springs, New York, May 3–7, 2009.

9. Z. WU et al., "Neutronics and Safety Studies on a Research Reactor Concept for an Advanced Neutron Source," *Nucl. Technol.*, **199**, *1*, 67 (2017); https://doi.org/10.1080/00295450.2017.1335146.

10. Y. ZHENG, L. SHI, and Y. DONG, "Thermohydraulic Transient Studies of the Chinese 200MWe HTR-PM for Loss of Forced Cooling Accidents," *Ann. Nucl. Energy*, **36**, *6*, 742 (2009); https://doi.org/10.1016/j.anucene.2009.02.007.

11. F. REITSMA, "The Pebble Bed Modular Reactor Layout and Neutronics Design of the Equilibrium Cycle," *Proc. Phys. of Fuel Cycles and Adv. Nuc. Syst.: Global Develop. (PHYSOR 2004)*, Chicago, Illinois, April 25–29, 2004.

12. A. XHONNEU, D. LAMBERTZ, and H.-J. ALLELEIN, "The Enhanced Fuel Management Models of the HTR

Code Package (HCP) Module SHUFLE," *Nucl. Eng. Des.*, **329**, 177 (2018); https://doi.org/10.1016/j.nucengdes.2017.11.042.

13. D. SHE et al., "PANGU Code for Pebble-Bed HTGR Reactor Physics and Fuel Cycle Simulations," *Ann. Nucl. Energy*, **126**, 48 (2019); https://doi.org/10.1016/j.anucene.2018.11.005.
14. J. ORTENSI and P. BALESTRA, "Initial Study on Cross Section Generation Requirements for a PBR Equilibrium Core," INL/EXT-21-64242, Idaho National Laboratory (2021).
15. E. TEUCHERT, U. HANSEN, and K. HAAS, "VSOP—Computer Code System for Reactor Physics and Fuel Cycle Simulation," *Kernforschungsanlage Jülich*, JÜL-1649 (Mar. 1980).
16. W. K. TERRY, H. D. GOUGAR, and A. M. OUGOUAG, "Direct Deterministic Method for the Deterministic Design, Analysis, and Optimization of the In-core Fuel Cycle of a Recirculating Pebble-Bed Reactor," *Ann. Nucl. Energy*, **29**, *11*, 1345 (2002); https://doi.org/10.1016/S0306-4549(01)00110-4.
17. C. LU et al., "Fully Ceramic Microencapsulated Fuel in Prismatic High Temperature Gas-Cooled Reactors: Analysis of Reactor Performance and Safety Characteristics," *Ann. Nucl. Energy*, **114**, 277 (2018); https://doi.org/10.1016/j.anucene.2017.12.021.
18. C. LU and N. R. BROWN, "Fully Ceramic Microencapsulated Fuel in Prismatic High-Temperature Gas-Cooled Reactors: Design Basis Accidents and Fuel Cycle Cost," *Nucl. Eng. Des.*, **347**, 108 (2019); https://doi.org/10.1016/j.nucengdes.2019.03.022.
19. E. BOMBONI et al., "Comparison Among MCNP-Based Depletion Codes Applied to Burnup Calculations of Pebble-Bed HTR Lattices," *Nucl. Eng. Des.*, **240**, *4*, 918 (2010); https://doi.org/10.1016/j.nucengdes.2009.12.006.
20. Y. NAGAYA et al., "MVP/GMVP II: General Purpose Monte Carlo Codes for Neutron and Proton Transport Calculations Based on Continuous Energy and Multigroup Methods," Japan Atomic Energy Research Institute (2005).
21. T. SETIADIPURA and T. OBARA, "Development of Monte Carlo–Based Pebble Bed Reactor Fuel Management Code," *Ann. Nucl. Energy*, **71**, 313 (2014); https://doi.org/10.1016/j.anucene.2014.04.010.
22. "MCNP—A General Monte Carlo N-particle Transport Code," Version 5, Los Alamos National Laboratory (2003).
23. M. FRATONI and E. GREENSPAN, "Equilibrium Core Composition Search Methodologies for Pebble Bed Reactors," *Nucl. Eng. Des.*, **166**, 1 (2010).
24. A. T. CISNEROS, "Pebble Bed Reactors Design Optimization Methods and Their Application to the Pebble Bed Fluoride Salt Cooled High Temperature Reactor (PB-FHR)," PhD Dissertation, Department of Nuclear Engineering, University of California, Berkeley (2013).
25. Y. WANG et al., "A Pebble Tracking Transport Algorithm for Pebble Bed Reactor Analysis," *Proc. PHYSOR 2018*, Cancun, Mexico, April 22–26, 2018.
26. Y. TANG et al., "Analysis of the Pebble Burnup Profile in a Pebble-Bed Nuclear Reactor," *Nucl. Eng. Des.*, **345**, 233 (2019); https://doi.org/10.1016/j.nucengdes.2019.01.030.
27. C. GARIAZZO, D. CHOJNOWSKI, and S. CHIRAYATH, "Nuclear Material Control and Accountancy Approach for Pebble Fueled Reactors Using a Novel Pebble-type Identification and Classification Technology," ANL/SSS-21/13, Argonne National Laboratory (2021).
28. E. J. MULDER and W. A. BOYES, "Neutronics Characteristics of a 165MWth Xe-100 Reactor," *Nucl. Eng. Des.*, **357**, 110415 (2020); https://doi.org/10.1016/j.nucengdes.2019.110415.
29. J. LEPPÄNEN et al., "The Serpent Monte Carlo Code: Status, Development and Applications in 2013," *Ann. Nucl. Energy*, **82**, 142 (2015); https://doi.org/10.1016/j.anucene.2014.08.024.
30. F. C. DIFILIPPO, "Monte Carlo Calculations of Pebble Bed Benchmark Configurations of the PROTEUS Facility," *Nucl. Sci. Eng.*, **143**, *3*, 240 (2003); https://doi.org/10.13182/NSE02-34.
31. Q. DAI et al., "Corrosion of Incoloy 800H Alloys with Nickel Cladding in FLiNaK Salts at 850°C," *Corros. Sci.*, **133**, 349 (2018); https://doi.org/10.1016/j.corsci.2018.01.026.
32. C. LU et al., "A Direct Comparison of High-Order and Low-Order Neutronics Calculations of the 165MWth Xe-100 Reactor," *Trans. Am. Nucl. Soc.*, **124**, *1*, 563 (2021); https://doi.org/10.13182/T124-35627.
33. "Equilibrium Core Concentrations," Kairos Power (2021); https://kairospower.com/generic-fhr-core-model/ (accessed Aug. 15, 2021).
34. E. J. MULDER, "VSOP-A: Code System for Simulating Aspects of the Reactor Physics and Fuel Cycle," MulTech Report MTR-001 (2019).